

Effects of Enlarged Surface / Volume Ratio in Solid Phase Assays

Documented on Basis of Thermo Scientific Nunc StarWell Module

Peter Esser, M.Sc., Senior Scientist, Thermo Fisher Scientific

Key Words

Thermo Scientific™ Nunc™ StarWell™, Thermo Scientific™ Nunc™ MaxiSorp™ MicroWell™ plate, Thermo Scientific™ Nunc™ MicroWell™ plate, ELISA, increased surface/volume ratio, short incubation time, geometric dimensions, advantages to the standard F-wells.

Goal

The goal of this application note is to describe the advantages of the Immuno C8 StarWell configuration. The surface area is increased up to a factor 1.52 compared to standard F-wells. This implies a faster adsorption so the assay time can be reduced and a higher signal will be obtained. Further to discuss the geometry and mathematic aspects of this special well configuration.

Thermo Scientific Nunc C8 StarWell Module consists of MicroWell reaction wells equipped with eight inside fins. As a result, the liquid covered surface area is increased by a factor ranging from 1.27 to 1.52, depending on the liquid volume (50 µL), when compared to standard, flat-bottom F-wells.

In a solid phase assay, e.g. ELISA, a larger surface to volume ratio implies a faster adsorption (immobilization) of molecules from the liquid phase.

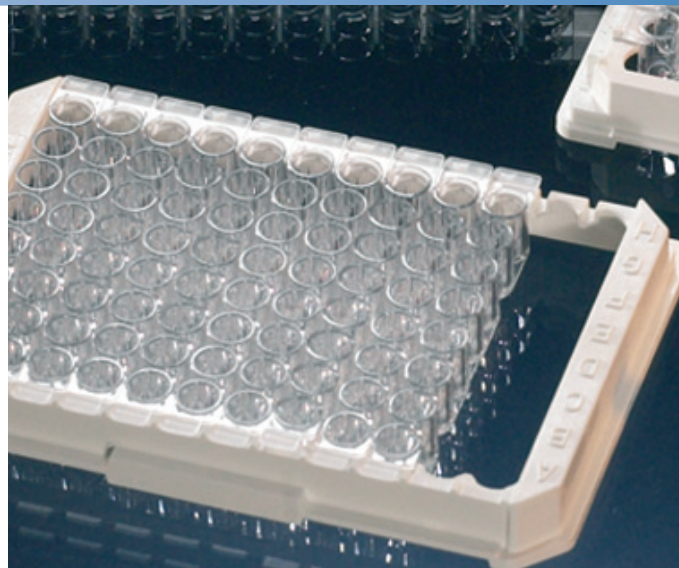
According to adsorption kinetics modelling 1, incubation times can be reduced by a factor equal to the square of the surface/volume increase factor, without reducing adsorption. Consequently, by using Nunc™ StarWell™ instead of F-well, incubation times can be reduced by a factor ranging from 1.6 to 2.3, depending on the liquid volume.

This article documents the StarWell versus F-well geometry and performance.

StarWell Geometry

The involved StarWell dimensions of interest are presented with the essential design in Fig. 1.

The key to StarWell geometry is the liquid height vs. volume relationship. However, the StarWell liquid heights cannot be determined by explicit calculation from the volumes. Therefore, the experimental StarWell to F-well OD relationship in Fig. 2 was utilized in conjunction with the calculated F-well liquid heights in Fig. 3, assuming



that the geometric heights are proportional to the OD readings.

In Fig. 3, the plot of the calculated ² F-well liquid heights (H^{\square}) vs. the respective volumes (V) was approximated by the line:

$$H^{\square} = 0.0282V + 0.2 \text{ mm} \quad \#1$$

In Fig. 2, the plot of the experimental StarWell to F-well OD ratios (OD^*/OD^{\square}) vs. the respective volumes in log-scale was found to be approximately linear by the equation:

$$OD^*/OD^{\square} = -0.22\log V + 1.55 \quad \#2$$

That is, for a given liquid volume, the StarWell liquid height is larger than the F-well liquid height by this factor due to the liquid displaced by the StarWell fins. Consequently, the StarWell liquid height (H^*) is determined by the product of #1 and #2:

$$H^* = (0.0282V + 0.2)^2 (-0.22\log V + 1.55) \text{ mm} \quad \#3$$

Fig. 1

Inner design and dimensions (in mm) of StarWell, seen from above (left), and in profile (right).

The fin front sides (a) are assumed to compensate for the parts of the “cylindrical” well surface occupied by the rear sides (b), whereas the parts of the well bottom occupied by the fin feet (c) remain uncompensated. Hence, if an estimated 0.06 cm² total feet area is taken from the flat bottom area of 0.33 cm², the fin net surface area is determined purely by the triangular fin sides (v) subtracted by the small, rounded corner “wings” (w), i.e. in total: $162(v-w) = 0.65 \text{ cm}^2$. Note that the free reading window between the fins fulfils the need for a minimum of a 4 mm diameter. The larger (bottom) distances of 1.75 mm between the fins along and across the longitudinal axis of the strip allow for access of common 1.6 mm instrumentation needles, aligned in these directions (e.g. Thermo Scientific Nunc Immuno Wash 8 and 12, Cat. Nos. 470173 and 455492).

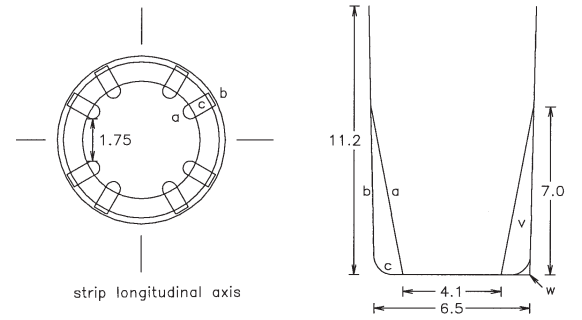
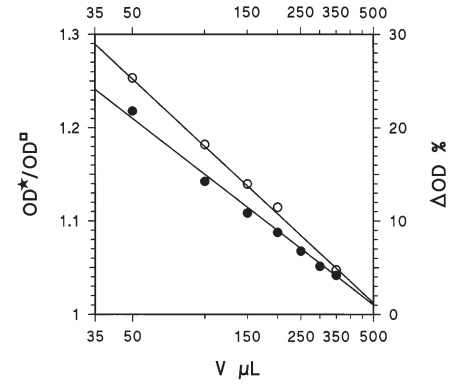


Fig. 2

StarWell to F-well OD ratio (OD^*/OD^\square), and corresponding increment (ΔOD), due to the StarWell fins' elevation of liquid heights, vs. volume (V). The measurements were made in “virgin” wells with converted peroxidase substrate solution, containing no detergent (●), or containing detergent (○). A downward liquid surface curvature was formed by presence of detergent, but not by absence of detergent. The semi-logarithmic plots were approximated by the straight lines according to the ratio equations #2 and #11, respectively. The application of #2, representing no curvature formation, is obviously the most relevant for geometric liquid height estimation. See text and Fig. 7 for further explanation.



yielding the total fin height = 7 mm when $V \approx 225 \mu\text{L}$, i.e. the volume just covering the fins. This equation was utilized to calculate the H^* values in Figs. 3 and 4, and in Table 1.

By fixing the StarWell bottom area (S_{bot}^*) at 0.27 cm² (Fig. 1), the fin surfaces' net area contributions are determined by their triangular sides, whose sum area (S_{fin}^*) at a given liquid height can be expressed by their total sum area = 0.65 cm², their total height = 7 mm, and the given liquid height (H^*):

$$S_{\text{fin}}^* = 0.652[10/7+(7-H^*)/10]2H^*/10 \text{ cm}^2 \quad \#4$$

yielding the maximum $S_{\text{fin}}^* = 0.65 \text{ cm}^2$ when $H^* = 7 \text{ mm}$, corresponding to $V = 225 \mu\text{L}$. Thus, for V up to 225 μL , the fin surfaces contribute with the area determined by #4, and for V above 225 μL , their contribution is constant = 0.65 cm².

The remaining StarWell surface area is determined by the covered cylindrical part of an F-well filled to the given height (H^*).

In Fig. 5, the plot of the calculated ² F-well surface areas (S^\square) vs. the respective volumes was approximated by the line:

$$S^\square = 0.0062V + 0.33 \text{ cm}^2 \quad \#5$$

By subtraction of the F-well bottom area = 0.33 cm² and insertion of $V = (H^\square - 0.2)/0.028$, derived from #1, this line transforms approximately to the analogous line:

$$S^\square - 0.33 = 0.2142H^\square \text{ cm}^2 \quad \#6$$

determining the cylindrical area of an F-well by the liquid height.

Consequently, the “cylindrical” area of a StarWell (S_{cyl}^*) is determined by replacing $S^\square - 0.33$ by S_{cyl}^* , and H^\square by H^* (determined by #3), in #6:

$$S_{\text{cyl}}^* = 0.2142H^* \text{ cm}^2 \quad \#7$$

The total area (S^*) of the liquid covered StarWell surface is finally determined by the sum of S_{bot}^* , S_{cyl}^* and S_{fin}^* (cf. #4):

$$S_{\leq 225}^* = 0.27 + 0.214TH^* + 0.65T[10/7 + (7-H^*)/10]TH^*/10 \text{ cm}^2 \quad \#8a$$

$$S_{\leq 225}^* = 0.27 + 0.214TH^* + 0.65 \text{ cm}^2 \quad \#8b$$

Fig. 3

Liquid height (H) vs. liquid volume (V), for StarWell (*), and for F-well (□). The H^{\square} calculations from ref. 2 were approximated by the straight line according to #1, and the H^* curve and selected values were calculated from #3. The red signed point corresponds to $H^* = 7.0$ mm for $V = 225 \mu\text{L}$, the volume just covering the StarWell fins (Fig. 4).

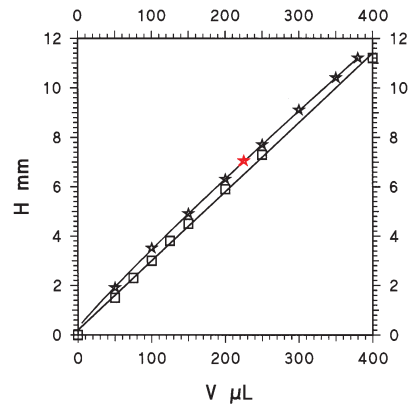


Fig. 4

Liquid heights (H) for selected liquid volumes (V), and bottom surface areas, for StarWell (left), and for F-well (right). The StarWell and F-well heights were calculated from #3 and #1, respectively, except the common total height, which is the measured well depth average. Note that the total StarWell liquid volume is less than the total F-well volume by $20 \mu\text{L}$, representing the StarWell fins' total liquid displacement.

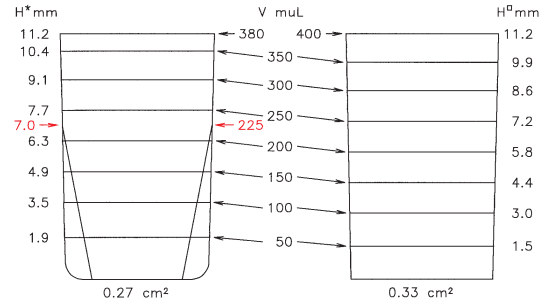


Table 1

StarWell parameters for selected liquid volumes (V). The figures written in red correspond to $V = 225 \mu\text{L}$, the volume just covering the StarWell fins. H^* = liquid height (#3). S^* = liquid covered surface area (#8a,b). ΔS = StarWell to F-well surface increment (#9). $P^* = S^*/V =$ surface/volume ratio. $\Delta P =$ StarWell to F-well surface/volume increment = ΔS for equal volumes. $\Delta T =$ possible minimum incubation time reduction (#10). $\Delta OD =$ StarWell to F-well OD reading increment due to the liquid height elevation (#12). $P^* \times 2K_{\text{IgG}} =$ surface saturating IgG concentrations for MaxiSorp (MS) and PolySorp (PS) surface qualities, where K_{IgG} stands for the MS and PS IgG adsorption capacities of 0.65 and $0.22 \mu\text{g}/\text{cm}^2$, respectively. For intermediate values is referred to the respective equations, or to interpolations in the respective figures. Note that the reading volume will be larger than the test volume, if an additional volume of enzyme inactivating solution is used.

V μL	H* mm	S* cm^2	S*/V P* cm^{-1}	ΔS ; ΔP %	ΔT %	ΔOD %	P* $\times K_{\text{IgG}}$ $\mu\text{g}/\text{ml}$	
							MS	PS
50	1.9	0.93	18.6	47	-54	25.2	12.1	4.1
100	3.5	1.41	14.1	52	-57	18.0	9.2	3.1
150	4.9	1.84	12.3	50	-56	13.8	8.0	2.7
200	6.3	2.24	11.2	46	-53	10.8	7.3	2.5
225	7.0	2.42	10.8	43	-51	9.5	7.0	2.4
250	7.7	2.57	10.3	40	-49	8.4	6.7	2.3
300	9.1	2.86	9.5	34	-44	6.5	6.2	2.1
350	10.4	3.15	9.0	29	-40	4.9	5.9	2.0
380	11.2	3.32	8.7	27	-38	4.1	5.7	1.9

Fig. 5

Liquid covered surface (S) vs. liquid volume (V) for StarWell (*), and for F-well (□). The S^{\square} calculations from ref. 2 were approximated by the straight line according to #5. The S^* curve and selected values were calculated from #8a,b by insertion of #3. The red signed point corresponds to the liquid covered StarWell surface area for $V = 225 \mu\text{L}$, the liquid volume just covering the StarWell fins.

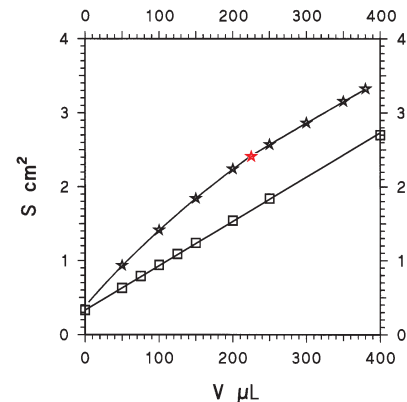


Fig. 6

StarWell to F-well increment (ΔS) of the liquid covered surface area, and minimum incubation time reduction (ΔT), vs. liquid volume (V). The selected values were calculated from #9 and #10, respectively, on the basis of #8a,b and #5, and the curves were visually fitted. The red signed points correspond to the respective values for $V = 225 \mu\text{L}$, the liquid volume just covering the StarWell fins. Note that the curves have numerical maxima at a volume around $100 \mu\text{L}$, consistent with the fact that the invariable bottom areas count more and more in the total areas with decreasing volume. Eventually, ΔS and ΔT change sign when the volume approximates zero, due to the larger F-well than StarWell bottom surface area, i.e., 0.33 cm^2 and 0.27 cm^2 , respectively (Fig. 1).

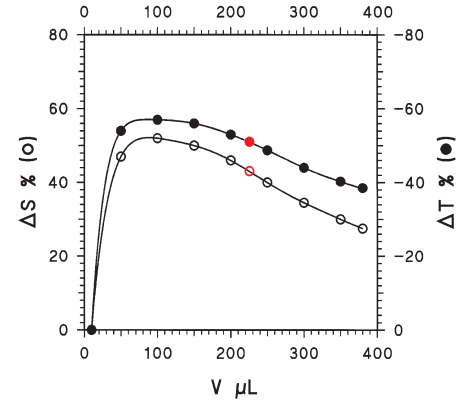
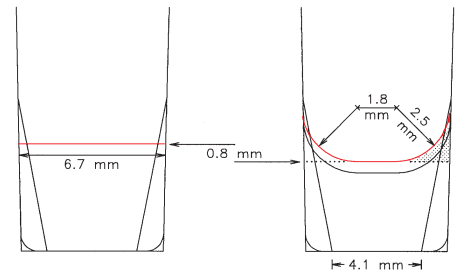


Fig. 7

Geometric liquid heights (left), and liquid heights determined by formation of a liquid surface curvature (right), estimated according to the text calculations, for $150 \mu\text{L}$ liquid volume in StarWell (red surface lines), and in F-well (black surface lines). The hatched area represents the assumed curvature profile enclosing the volume corresponding to the liquid height difference of 0.8 mm , when rotated 360° along the well circumference. Note that the plane reading area diameter is reduced from 4.1 mm (of the well bottom reading window) to about 1.8 mm of the liquid surface due to the curvature formation. See text and Fig. 2 for further explanation.



where $S^*_{\leq 225}$ is valid for $H^* \leq 7 \text{ mm}$ (or $\leq 225 \mu\text{L}$), and $S^*_{\leq 225}$ is valid for $H^* \leq 7 \text{ mm}$ (or $V \leq 225 \mu\text{L}$). By insertion of H^* , determined by #3, these equations determine S^* by the volume, and were utilized as such to calculate the S^* values in Fig. 5 and Table 1.

Further, the StarWell to F-well area increment (ΔS %), equal to the surface to volume increment (ΔP %) for equal volumes, and the possible (minimum) incubation time reduction (ΔT %), (cf. StarWell Performance below), are determined by the ratio between #8a,b and #5 for discrete volumes:

$$\Delta S = 100T(S^*/S^{\square}-1) \% \quad \#9$$

$$\Delta T = -100T[1-1/(S^*/S^{\square})^2] \% \quad \#10$$

These equations were utilized to calculate the ΔS and ΔT values in Fig. 6 and Table 1.

Geometry Discussion

The geometric liquid heights may not be identical with the real heights due to formation of a liquid surface curvature (Fig. 2). This has implications for the real liquid covered surface areas and for the reading liquid heights. See Fig. 7.

The formation of a liquid surface curvature depends on the liquid composition, especially the presence of detergent, as well as on the well surface character. With a

standard 0.05% detergent content in the liquid, or after a standard, three layer IgG sandwich procedure, a liquid surface curvature is formed. Therefore, the data in Fig. 2, obtained by presence of detergent ($OD^*/OD^{\square}_{\text{det}}$), may represent the most likely StarWell to F-well OD increase that would be experienced in the majority of cases. These data were approximated by the equation:

$$OD^*/OD^{\square}_{\text{det}} = -0.242\log V + 1.66 \quad \#11$$

corresponding to the increment:

$$\Delta OD = (-0.2422\log V + 1.66 - 1) 2100\% \quad \#12$$

Thus, equation #12 was utilized to calculate the OD values in Table 1.

The liquid surface curvature was estimated considering $150 \mu\text{L}$ liquid volume, at which the geometric heights are 4.9 and 4.4 mm for StarWell and F-well, respectively (Fig. 4). With a liquid surface curvature, the reading heights are lower than these geometric heights by a distance, d , determined by the $OD^*/OD^{\square}_{\text{det}}$ value = 1.138 , calculated from #11 for $V = 150 \mu\text{L}$: $(4.4-d)21.138 = 4.9-d$, implying $d \approx 0.8 \text{ mm}$. By enclosing the corresponding volume difference, $0.82\pi 23.35^2 \mu\text{L}$, in a well-inscribed rotation body with a profile area, $r^2 X(1-\pi/4) \text{ mm}^2$ (Fig. 7), the curvature estimate resulted from the calculated radius, $r \approx 2.5 \text{ mm}$, in that profile. This leaves a plane reading area diameter of only 1.8 mm , giving occasion for a general consideration of the reading beam widths and center positions.

StarWell Performance

For simplicity, the demonstration of StarWell vs. F well performance was based on one-layer adsorption experiments.

StarWells (*) and F-wells (□) of Thermo Scientific Nunc MaxiSorp surface quality (Cat. Nos. 441653 and 468667) were incubated for increasing times with 150 μL /well of peroxidase conjugated IgG = IgG:HRP (Dako P 128), 0.05 $\mu\text{g}/\text{mL}$, or 1xIgG:HRP + 99xIgG (Dako Z 181), 5 $\mu\text{g}/\text{mL}$, both in carbonate buffer, pH 9.6. After adsorption, the wells were washed three times with PBS containing an extra 0.2 M NaCl and 0.05% Triton X-100, pH 7.2. This was followed by substrate reaction with 150 μL /well of $\text{H}_2\text{O}_2/\text{OPD}$ in phosphatecitrate buffer, pH 5.0, subsequently stopped with 110 μL /well of 2 N H_2SO_4 , resulting in 260 μL reading volumes.

All reactions were performed at room temperature. The OD readings are presented in Fig. 8.

According to the estimated MaxiSorp IgG adsorption capacity of $650 \text{ ng}/\text{cm}^2$, the IgG concentrations utilized correspond to 1% and 100% F-well surface saturation, i.e. $F^\square = 0.01$ and 1, respectively. Using 150 μL reagent volumes, the corresponding StarWell values are $F^* = 0.00667$ and 0.667, respectively, since the StarWell surface increase factor is 1.50 (Table 1). [F generally denotes the ratio between the number of supplied molecules and the number of molecules that the surface can adsorb - not to be confused with the designation “F-well” for the standard, flat-bottom MicroWell.] Further, the F-well and StarWell surface/volume ratios are $P^\square = 8.3 \text{ cm}^{-1.2}$ and $P^* = 8.321.5 \text{ cm}^{-1}$, respectively.

To match the StarWell readings with the F-well readings for a comparative adsorption analysis, the StarWell readings were corrected for the elevated liquid heights by division with the $\text{OD}^*/\text{OD}^\square_{\text{det}}$ value = 1.08, calculated from #11 for $V = 260 \mu\text{L}$.

The corrected readings were simulated in Fig. 9 by the model Adsorption Density Equations (ADE), #14a,b in Appendix, showing correlation between real and theoretical adsorption kinetics.

As an example, the levels of 75% adsorption of supplied molecules were used for further comparison of the StarWell vs. F-well adsorption performance (Fig. 9).

In Fig. 10, the model Adsorption Time Equations (ATE), #15a,b,c in Appendix, were depicted for 75% adsorption of the supplied molecules with StarWell and with F-well, respectively. The graphs illustrate the time reductions obtainable by utilization of StarWell instead of F-well in accordance with the interpolations in Fig. 9.

At concentrations corresponding to $\leq 1/10$ F-well surface saturation, i.e. $0 < F^\square \leq 0.1$, the time reduction is almost constant by a factor equal to the square of the surface to volume ratio increase. The constancy is due to the fact that in this F regime plenty of unoccupied sites remain available on the surfaces.

At higher concentrations, the time reduction is increasingly larger with a maximum at the concentration

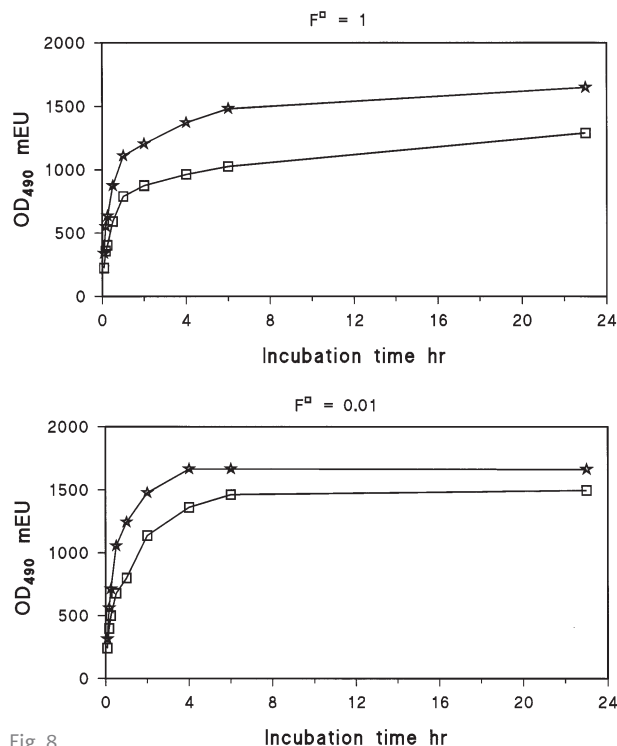


Fig. 8

IgG adsorption kinetics data from incubation of MaxiSorp StarWell (*) and MaxiSorp F-well (□) with 150 μL /well of IgG solutions with concentrations corresponding to 1% F-well surface saturation, i.e. $F^\square = 0.01$ (above), and to 100% F-well saturation, i.e. $F^\square = 1$ (below). See text for further explanation.

just matching the F-well surface saturation, i.e. $F^\square = 1$. This can be explained by considering that it will take additional time for the last molecules to find the last unoccupied spaces on the surface.

At still higher concentrations, i.e. $F^\square > 1$, the situation is eventually reversed. That is, more time is required with StarWell than with F-well to adsorb e.g. 75% of the supplied molecules. However, in this F regime adsorption times become very short in any case.

In Fig. 11, the model StarWell to F-well Adsorption Increment Equations (AIE), #16a,b in Appendix, expressing the adsorption increment as a function of the time reduction, were depicted for various F-well adsorption percentages. The graphs illustrate that the StarWell adsorption increment increases with decreasing F-well adsorption percentage and with increasing F^\square , in accordance with the ADE curves in Fig. 9.

Performance Discussion

The StarWell to F-well performance relationship holds for immobilization of any reactant in a solid phase bioassay sequence ¹, because, when other things are equal, it results purely from the larger StarWell probability that a molecule will hit the surface due to the larger surface to volume ratio (i.e. the liquid is exposed to more surface).

The primary performance aspect of StarWell is incubation time saving. This can be converted to an immobilization increase by renouncing all, or part of, the possible time reduction, as illustrated in Fig. 11. Therefore, some increase of sensitivity could be gained within a finite incubation time.

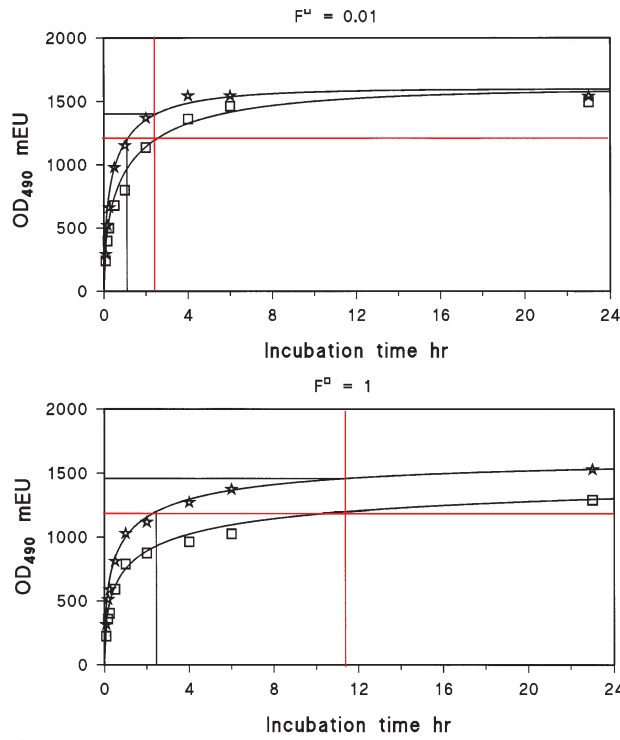


Fig. 9

Simulations of the data in Fig. 8 by the model ADEs (#14a,b) for F^{\square} ; $F^* = 0.01$; 0.00667 (above), and for F^{\square} ; $F^* = 1$; 0.667 (below). The model adsorption densities (E_t) were converted to ODs by multiplication with the common maximum signal estimate of 1600 mEU, divided by the respective F values. The StarWell data were corrected for the liquid height elevations according to #11 for 260 μL reading volumes. As an example, the levels of 75% adsorption of supplied molecules (red horizontal lines) were used for comparison of the StarWell vs. F-well performance. Between the line of equal adsorption percentage (75%) and equal incubation time (red vertical line) in each diagram, the respective StarWell curves exhibit regimes, demarcated by the black lines, where both time reduction and adsorption increase can be obtained. Note that the StarWell adsorption acceleration is much larger at the high molecular supplies than at the low supplies. See text and Figs. 10 and 11 for further explanation.

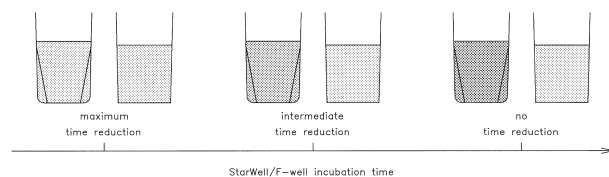


Fig. 12

Summarizing illustration, for 250 μL reading volume, of the advantages with StarWell, in relation to F-well incubated for less than the time required to immobilize “all” the supplied molecules (for $F^{\square} \leq 1$). At “maximum” incubation time reduction with StarWell, i.e. the reduction determined by the surface to volume ratio increase, the same amount of molecules will be immobilized, resulting in the same concentration of signal molecules, in both wells (left). At no time reduction with StarWell, a “maximum” immobilization enhancement will occur, resulting in a larger concentration of signal molecules (right). At an intermediate time reduction, an intermediate immobilization enhancement will occur, resulting in an intermediate concentration of signal molecules (middle). Note that the reading column height enlargement with StarWell will add to the OD reading in any case.

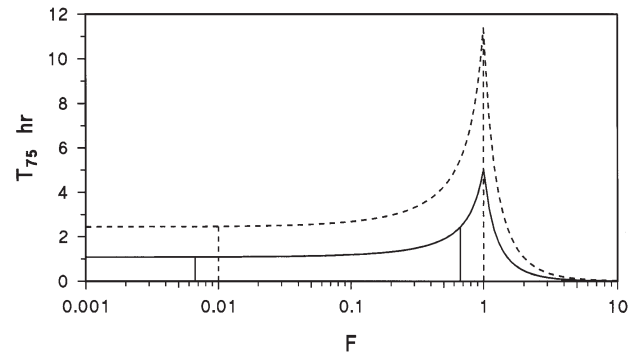


Fig. 10

Graphic presentation of the model ATEs (#15a,b,c) for 75% adsorption of the supplied molecules (Fig. 9), i.e. the 75% adsorption time (T_{75}) vs. the ratio (F) between the number of supplied molecules and the number of molecules that the surface can adsorb, for StarWell (---), and for F-well (---). For $F^* = F^{\square}$ (implying different StarWell and F-well concentrations of supplied molecules), the $T_{75}^{\square}/T_{75}^*$ ratio is constant $= 1.50^2 = 2.25$ in the whole F regime, $0 < F < \infty$. For equal concentrations (implying $F^* = 0.667 \times F^{\square}$), the $T_{75}^{\square}/T_{75}^*$ ratio is approximately constant ≈ 2.3 for $0 < F^{\square} \leq 0.1$, and increasingly larger for $0.1 < F^{\square} \leq 1$ with a maximum $= 4.7$ (calculated from #15a,b) for $F^{\square} = 1$. The solid and dashed vertical lines represent, respectively, the T_{75}^* and T_{75}^{\square} times for the actual F values. Note that these times are, respectively, the same as the interpolated times in Fig. 9. See text for further explanation.

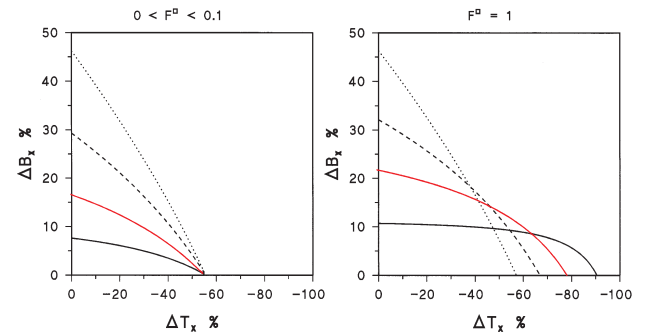


Fig. 11

Graphic presentation of the model AIEs (#16a,b), i.e. StarWell to F-well adsorption increment (ΔB_x) vs. time reduction (ΔT_x), corresponding to the data simulations in Fig. 9, for F-well adsorption percentages, $x = 10\%$ (···), 50% (---), 75% (-·-·-) and 90% (----). For $0 < F^{\square} \leq 0.1$ (above), ΔB_x increases with decreasing x , whereas ΔT_x is approximately constant for any x . For $F^{\square} = 1$ (below), ΔB_x increases further with decreasing x , and ΔT_x now increases with increasing x . For $0.1 < F^{\square} < 1$, there will be a gradual transition from the upper to the lower diagram curves. Note that between the extremes of maximum ΔT_x (for $\Delta B_x = 0$) and maximum ΔB_x (for $\Delta T_x = 0$), intermediate ΔT_x and ΔB_x can be obtained.

However, using enough incubation time, virtually all (scarce) analyte molecules in a certain liquid volume will eventually be immobilized in both wells, since there will normally be ample binding sites present on both well surfaces. This can be illustrated by the analyzed system, regarding the IgG as the analyte to be “captured” by the adsorbing surface sites.

For concentrations corresponding to, for example, $F^{\square} \leq 0.01$, the F-well incubation time required to obtain 99% adsorption is almost constant ≈ 6 hr, calculated from #15a (Appendix) for $F^{\square} = 0$. Thus, using this incubation time, practically no additional adsorption will be obtained with StarWell; however, the same adsorption could have been obtained in about half the time, i.e. ≈ 3 hr.

A true sensitivity increase can be obtained with StarWell only when the analyte binding molecules are so poor that they are a limiting factor to analyte immobilization. Such poor binding characteristics could be observed in any solid phase system.

It should be noted that a prerequisite for maintenance of the StarWell effects on a second layer analyte immobilization is that the surface coating densities in StarWell and F-well are equal, implying a proportionally higher StarWell coating concentration. Thus, it can be derived from the model ¹ that the analyte immobilization times will just balance by using the same coating concentration (\leq the F-well saturating concentration) in both wells, implying a proportionally lower StarWell coating density.

If a certain sub-saturating coating density is desirable for some reason (cf. the following article), rather than a saturating density, an inherent delay of analyte immobilization could be remedied, to some extent at least, by using StarWell instead of F-well.

In addition to faster immobilization of liquid phase molecules, the vertical MicroWell reading configuration results in larger OD readings in StarWell than in F-well. This is due to the fins' elevation of liquid heights (cf. StarWell Geometry). If, for instance, the height dependent StarWell to F-well OD increment is 10%, there will, for this reason alone, be 10% more distance between the signal and the background readings with StarWell. This effect would obviously be the more pronounced as the reading volume is reduced (Table 1).

The advantages of StarWell compared to F-well, comprising immobilization time reduction, immobilization enhancement, and reading column height enlargement, are summarized qualitatively in Fig. 12.

References

1. Esser P. (1992).
The surface/volume ratio in solid phase assays.
Thermo Scientific Nunc Application Note No 10B.
2. Esser P. (1985).
Adsorption geometry in Nunc products for solid phase assays.
Thermo Scientific Nunc Application Note No 1.
3. Esser P. (1988).
Principles in adsorption to polystyrene.
Thermo Scientific Nunc Application Note No 6A.

Appendix

The adsorption kinetics model ¹ originates in a combination of diffusion kinetics with the kinetics for a second order chemical reaction (A+C ⇌ B), regarding the adsorbing surface sites as one reactant (A), the liquid phase molecules as the other reactant (C), and the bound molecules as the reaction product (B), to form the Adsorption Rate Equation (ARE), (cf. symbol legend below):

$$dB_t/dt = [(A-B_t)/A] \cdot [(C-B_t)/V] \cdot S \cdot (k \cdot D/\pi)^{1/2} \cdot t^{-1/2} \quad \#13$$

which by integration gives the Adsorption Density Equations (ADE), expressing the fraction, E_t , of the surface adsorption capacity adsorbed at time t :

$$E_t \{F \neq 1\} = \frac{B_t}{A} = \frac{1 - \exp\{(F-1) \cdot P \cdot (4 \cdot k \cdot D/\pi)^{1/2} \cdot t^{1/2}\}}{1/F - \exp\{(F-1) \cdot P \cdot (4 \cdot k \cdot D/\pi)^{1/2} \cdot t^{1/2}\}} \rightarrow \begin{cases} F \text{ for } F < 1 \\ 1 \text{ for } F > 1 \end{cases} \quad \#14a$$

$$E_t \{F=1\} = P \cdot (4 \cdot k \cdot D/\pi)^{1/2} \cdot t^{1/2} / [P \cdot (4 \cdot k \cdot D/\pi)^{1/2} \cdot t^{1/2} + 1] \rightarrow 1 \quad \#14b$$

From equations #14a,b, one can derive the Adsorption Time Equations (ATE), expressing the time, T_x , required to adsorb $x\%$ of the supplied molecules (for $F \leq 1$), or $x\%$ of the surface adsorption capacity (for $F > 1$):

$$T_x \{F < 1\} = P^{-2} \cdot (4 \cdot k \cdot D/\pi)^{-1} \cdot (1-F)^{-2} \cdot [\ln\{(100-x)/F\} / (100-x)]^2 \text{ hr} \quad \#15a$$

#15b

$$T_x \{F > 1\} = P^{-2} \cdot (4 \cdot k \cdot D/\pi)^{-1} \cdot (1-F)^{-2} \cdot [\ln\{(100-x)/F\} / (100-x)]^2 \text{ hr} \quad \#15c$$

From equations #15a, b, one can derive the Adsorption Increment Equations (AIE), expressing e.g. the StarWell to F-well adsorption increment, ΔBX , when the F-well adsorption is $x\%$ of the supplied molecules:

$$\Delta BX \{F^\square < 1\} = [100 \cdot \frac{\{(1 - |\Delta TX| / 100)^{1/2} \cdot (p - F^\square) / (1 - F^\square)\}}{1 - \{(100-x \cdot F^\square) / (100-x)\}} - x] \cdot 100/x \% \quad \#16a$$

$$\Delta BX \{F^\square = 1\} = [100 \cdot \frac{p \cdot 1 - \exp\{(1 - |\Delta TX| / 100)^{1/2} \cdot (p-1) \cdot x / (100-x)\}}{1/p - \exp\{(1 - |\Delta TX| / 100)^{1/2} \cdot (p-1) \cdot x / (100-x)\}} - x] \cdot 100/x \% \quad \#16b$$

The used symbols translate as follows:

A = number of molecules that the surface can adsorb	F^\square = F-well F value
B_t = number of molecules adsorbed at time t	k = dimensionless coefficient = 2π
ΔB = StarWell to F-well adsorption increment = %	P = $S/V = \text{cm}^{-1}$
C = number of supplied molecules	p = P^*/P^\square
D = diffusion constant of IgG = $1.44 \cdot 10^{-3} \text{ cm}^2 \cdot \text{hr}^{-1}$	S = liquid covered surface area = cm^2
E_t = fraction of A adsorbed at time t	t = elapsed adsorption time = hr
F = C/A	ΔT = StarWell to F-well adsorption time reduction = %
	V = liquid volume = cm^3

thermoscientific.com/diagnosticplates

© 2015 Thermo Fisher Scientific Inc. All rights reserved. All trademarks are the property of Thermo Fisher Scientific Inc. and its subsidiaries.

Asia: Australia: 1300-735-292; New Zealand: 0800-933-966; China +86-21-6865-4588 or +86-10-8419-3588; China Toll-free: 800-810-5118 or 400-650-5118; Singapore +65-6872-9718; Japan: +81-3-5826-1616; Korea +82-2-2023-0640; Taiwan +886-2-87516655; India: +91-22-6680-3000 **Europe:** Austria: +43-1-801-40-0; Belgium: +32-2-482-30-30; Denmark: +45-4631-2000; France: +33-2-2803-2180; Germany: +49-6184-90-6000; Germany Toll-free: 0800-1-536-376; Italy: +39-02-95059-554; Netherlands: +31-76-571-4440; Nordic/Baltic/CIS countries: +358-10-329-2200; Russia: +7-(812)-703-42-15; Spain/Portugal: +34-93-223-09-18; Switzerland: +41-44-454-12-12; UK/Ireland: +44-870-609-9203

North America: USA/Canada +1-585-586-8800; USA Toll-free: 800-625-4327

South America: USA sales support: +1-585-586-8800 **Countries not listed:** +49-6184-90-6000 or +33-2-2803-2000

Thermo
SCIENTIFIC

A Thermo Fisher Scientific Brand